Opt Quant Electron (2017) 49:4
DOI 10.1007/s11082-016-0839-9

Effect of aluminum nanoparticles on the linear and nonlinear optical properties of PVA

Fatemeh Naseri[1] · **Davoud Dorranian**[1]

Received: 28 June 2016 / Accepted: 25 November 2016 / Published online: 9 December 2016

Abstract Linear and nonlinear optical properties of Polyvinyl Alcohol thin film doped with aluminum nanoparticles have been investigated experimentally. Aluminum nanoparticles were produced using pulsed laser ablation method. The fundamental wavelength of Nd-YAG laser at 7 ns pulse width was employed to produce aluminum nanoparticles in water at different sizes and concentrations. TEM images were used to study the nanoparticles after ablation. UV–Vis–NIR spectroscopy data were used to extract the real and imaginary parts of refractive index and dielectric functions of films and z-scan technique was used to measure the nonlinear refractive index and absorption coefficient of films. Results show that in comparison with particle size, the concentration of doped nanoparticles is more effective on the optical properties of polymers thin films. Band gap energy of polymer films was decreased with decreasing the size and increasing the concentration of nanoparticles while their refractive index was decreased.

Keywords Polymer · Nanoparticles · Aluminum nanoparticle · Laser ablation · Linear optics · Nonlinear optics · Z-scan technique · Bandgap energy

1 Introduction

Research into the synthesis and applications of nanoparticles (NPs) is currently intense due to their wide range of potential applications in the biomedical, optical, and electronic fields. Nanomaterials, defined as materials having typical dimensions less than 100 nm, present very special physical and chemical properties that strongly depend on their size and shape (Abbasi and Dorranian 2015). Those significant properties of NPs, such as their

✉ Davoud Dorranian
doran@srbiau.ac.ir

[1] Laser Laboratory, Plasma Physics Research Center, Science and Research Branch, Islamic Azad University, Tehran, Iran

chemical, electronic, mechanical, and optical properties, obviously distinguish them from those of the bulk of these materials. NPs colloids in solution have been studied extensively because of their large third-order nonlinear susceptibilities and nonlinear optical response. Among the various NPs available, nanocrystalline materials have gained importance in recent years, as they represent a class of material with new exciting properties and wide technological applications such as photocatalysis, chemical remediation, photoinitiation of polymerization reactions, quantum dot devices and solar energy conversion (Ganeev et al. 2002). Researching on the new nanomaterials for optical photonics devices spreading over a large area of studies on nonlinear materials has become a major research area. Also, nonlinear properties of organic material have widely studied under the search for nonlinear optical material with large nonlinearities, they are imperative for potential application in optical limiting and modern optical devices. Polymeric materials have specific properties such as high flexibility, and low density. Therefore, these materials have various industrial applications. As a result, one of the most significant ways to find material with noticeable nonlinear absorption coefficients or refractive index is based on NPs doped on polymers. When NPs are embedded in a polymer matrix, the linear and nonlinear optical properties of the nanocomposite films can be different from those of the pure polymer and NPs.

Aluminum NPs are considered as a possible fuel advanced energetic materials applications such as propellants and pyrotechnics, as they feature high surface area which provides enhanced heat release during their exothermal oxidation (Park et al. 2005; Galfetti et al. 2006; Tyagi et al. 2008). Therefore, Aluminum nanostructures have recently attracted interest as building blocks for high-capacity hydrogen storage materials (Roach et al. 2009; Balde et al. 2008; Zheng et al. 2008); this is due to the ability of metallic Aluminum to form Hydrogen upon reaction with water. Consequently, Aluminum NPs have unique optical characteristics for optoelectronic applications. Polyvinyl alcohol (PVA) is a semicrystalline polymer, which may be a suitable host material due to its good thermostability, chemical resistance, high mechanical strength (film forming), water solubility, moderate and dopant dependent electrical conductivity along with its consideration among the best polymers as host matrix for Aluminum NPs (Fussell et al. 2005). It is an important material with various applications, which is used in different field of science and technology. There are strong interactions between the polymer chains of PVA, which are attributable to the formation of hydrogen bonds between the hydroxyl groups. Metal NPs doped in polymers attracts great consideration; hence, the widened application goal offered by these hybrid materials. Liu et al. (2009) showed that the crystal structure of PVA changes after the formation on a composite with NPs. For their application in optoelectronic, electrical, and optical devices, biomedical science, and so forth, main key points are selection of polymer-metal NPs combination, controlling the particles size, their concentration, and distribution within the polymer matrix (Weickmann et al. 2005; Keirbeg and Vollmer 1995; Chen and Sommers 2001). Chemical structure of PVA is illustrated in Fig. 1a.

Many different methods have been developed for the preparation of colloidal solutions of NPs, such as chemical reaction, sol–gel, physical vapor deposition (PVD), chemical vapor deposition (CVD), and pulsed laser ablation (PLA) methods (Yang 2007). Compared with conventional chemical methods, the PLA methods performed in liquids are clean and they do not need any catalysts or complex susceptibilities and the products usually require no further purification. In addition, the size and shape of NPs can be approximately controlled by altering the laser energy and ambient temperature in this method (Yang 2007).

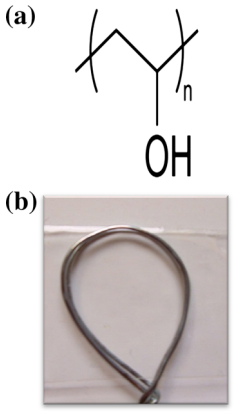

Fig. 1 **a** Chemical structure of PVA, **b** the colorless PVA film

Nonlinear optical techniques are important for materials research due to their high sensitivity to the molecular properties of the system (Yano et al. 1997; Porel et al. 2007; Sheik-Bahae and Hasselbeck 2000). A collective effort from physicists, chemists and material scientists is currently in progress to understand the fundamental relationships between the optical response and the molecular structure in polymers. The simplest method to measure the nonlinear optical properties of materials is Z-scan method. Z-scan is a well-established method for the determination of nonlinear refraction and absorption and has been widely used in material characterization since it can provide not only the magnitudes of real and imaginary parts of nonlinear susceptibility, but also their signs (Yang et al. 2004; Catunda et al. 1986; Tingchao et al. 2008; He et al. 1997). In this method, the sample is scanned along the propagation path of a focus the Gaussian laser. The physical properties of a polymer are strongly dependent on the size or length of the polymer chain. In π-conjugated organic compounds (polymers and oligomers), electron can move in large molecular orbitals.

In this study we used ultraviolet visible near infrared (UV–Vis–NIR) spectroscopy, transmission electron microscopy (TEM) analysis. Then single z-scan method is employed to investigate the NLO properties of samples. We have experimentally investigated linear absorption measurement using a low-power laser and nonlinearities including nonlinear absorption and nonlinear refractive index.

Single-beam Z-scan technique performed with the 532 nm, laser light generated from a low power continues wave (CW) Nd-YAG laser source, serving as the excitation beam.

2 Experimental

Three samples of Al NPs were prepared using 2, 2.5, and 3 J/cm^2 fluences of a pulsed Nd:YAG laser of 7 ns pulsed width, and 1064 nm wavelength to irradiate high purity Al target in distilled water. Repetition rate of laser pulse was 10 Hz. The spot size of the beam was 6 mm before lens. A 80 mm focal length lens was used to focus the laser beam on the Al target. Height of deionized water on the aluminum target was 5 mm. Aluminum target was ablated with 500 laser pulses at different energies. Detail about the sample preparation is presented in Table 1. The Al suspension samples were colorless after ablation.

Table 1 Comparison of the value of L_{eff}, ΔT_{P-V}, $\Delta\varphi$, n_0, and E_g of samples

Sample	Intensity (J/cm^2)	ΔT_{P-V}	$L_{eff} \times 10^{-2}$ (mm)	$\Delta\varphi$	n_0	E_g
PVA	–	0.6327	6.48	1.8533	1.954	5.01
Sample 1	2	0.5504	5.89	1.6122	1.908	4.89
Sample 2	2.5	0.5057	5.69	1.4813	1.889	4.78
Sample 3	3	0.4448	5.37	1.3029	1.82	4.69

PVA film were prepared by solving 1 g of commercial PVA powder in 20 ml distilled water and stirred for 2 h at 57 °C temperature. In the second step 10 ml of Al suspension was added into 20 ml of PVA solution and again stirred for 1 h at room temperature. To make Al NPs doped PVA thin films, samples were then poured on a flat plate and dried at the room temperature for 24 h. The thickness of films was 0.07 mm. One sample was made without any Al NP. Since Al nanoparticle suspensions and PVA polymer were colorless, Al nanoparticle doped PVA film was also colorless which is shown in Fig. 1b.

UV–Vis–NIR spectrum (PG instrument, T80), TEM micrographs (Philips EM 208), were used to study the morphology and structure of Al NPs (Fig. 2).

The transmission and reflection spectrum of film samples were measured using a Varian carry 500 UV–Vis–NIR spectrophotometer.

The nonlinear optical properties of Al/PVA nanocomposite films were measured by using the Z-scan technique. Based on the method developed by Sheik-Bahae et al. (2000). The experimental setup of Z-scan experiment is shown in Fig. 3. The excitation source in our experiment was the second harmonic beam of a continuous wave (CW) Nd-YAG laser at 532 nm wavelength. In the experimental setup of Fig. 3, the laser beam of 2.55 mm diameter after propagating through a beam splitter was focused by a 10 cm focal length lens on the polymer target, leads to Rayleigh length of $Z_0 = 2.6$ mm. The output beam power of the laser was 62 mW. Two power meters were used to measure the incident and transmitted power of laser beam. Movement of sample or detector in the experiment was done using a micrometer translating stage. The distance between the lens focal point as the origin and power meter was changed from -10 mm before of focal lens and $+10$ mm after that during the experiment. The pinhole was 0.8 mm in diameter.

3 Results and discussion

TEM images of Al nanoparticle suspensions in distilled water are presented in Fig. 2. For taking TEM pictures a drop of the suspension containing nanoparticles is deposited and dried on a carbon-coated copper grid. Beside each image in Fig. 2, the particle size distribution of Al nanoparticles, obtained from TEM analysis is plotted using measurement software. As can be seen, the Al nanoparticles are almost spherical in all samples. Aggregation was increased from sample 1 to 3. With increasing the laser fluence, the average size of the spherical nanoparticles was decreased while their concentration increased noticeably. Average size of nanoparticles extracting from TEM images are 19, 11, and 9 nm for samples 1–3 respectively.

The variation of transmittance (T) and reflectance (R) of Al doped PVA films as a function of wavelength for samples 1–3 was recorded at room temperature and is showed

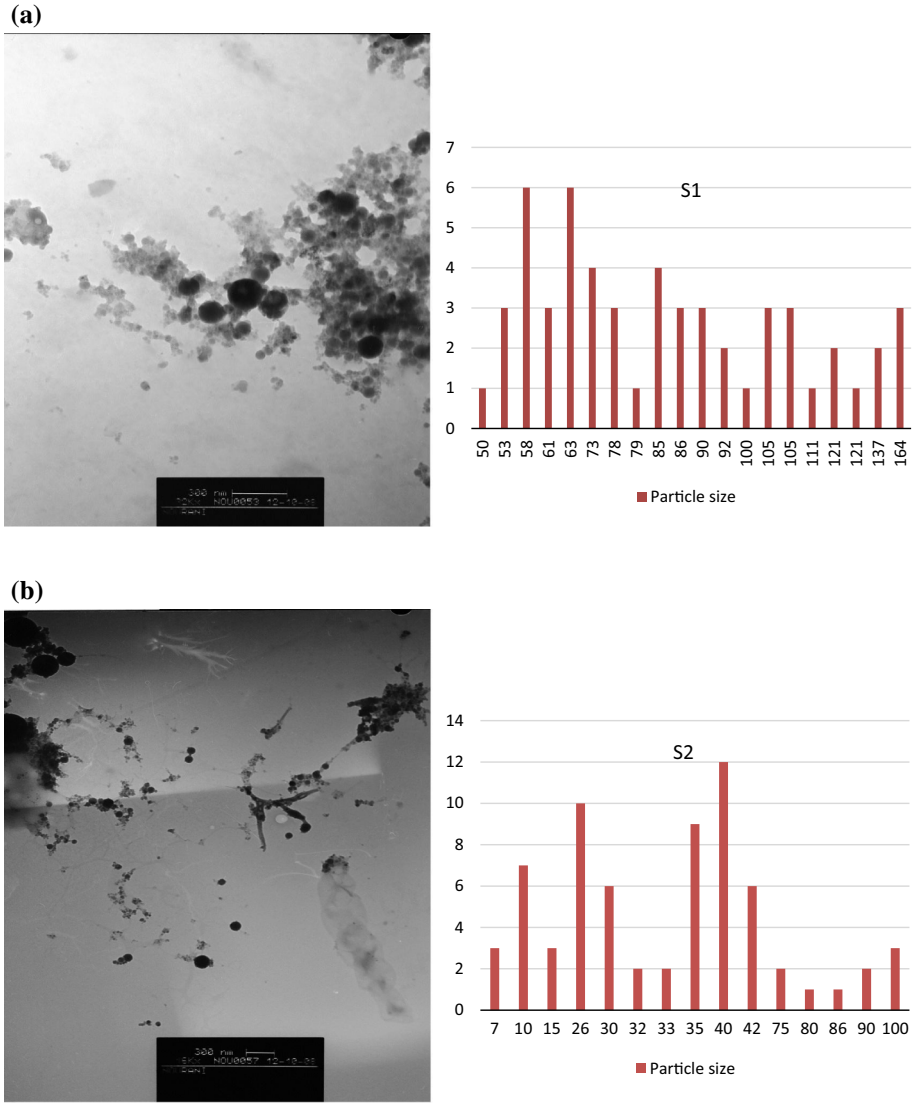

Fig. 2 TEM images, **a** S1 (1.5 J/cm^2), **b** S2 (2 J/cm^2), **c** S3 (3 J/cm^2)

in Fig. 4a and the refractive index of samples in UV–Vis–NIR region is presented in Fig. 4b. To observe the effect of doping in the transmission and reflection spectrum, the transmission and reflection spectrum of pristine PVA film is also plotted in these figures. Pure PVA is a colorless polymer without any noticeable absorption in the visible range. The sharp increase observed in transmittance spectrum in the range of 210–248 nm is due to the presence of the PVA polymer bandgap (Yang 2007). Doping Al nanoparticles in PVA film leaded to decrease the transmittance of the film. The same was occurred for the reflectance spectrum. Reflectance of doped films was decreased from pristine PVA film and from sample 1 to 3. This is the effect of linear absorption of doped nanoparticles.

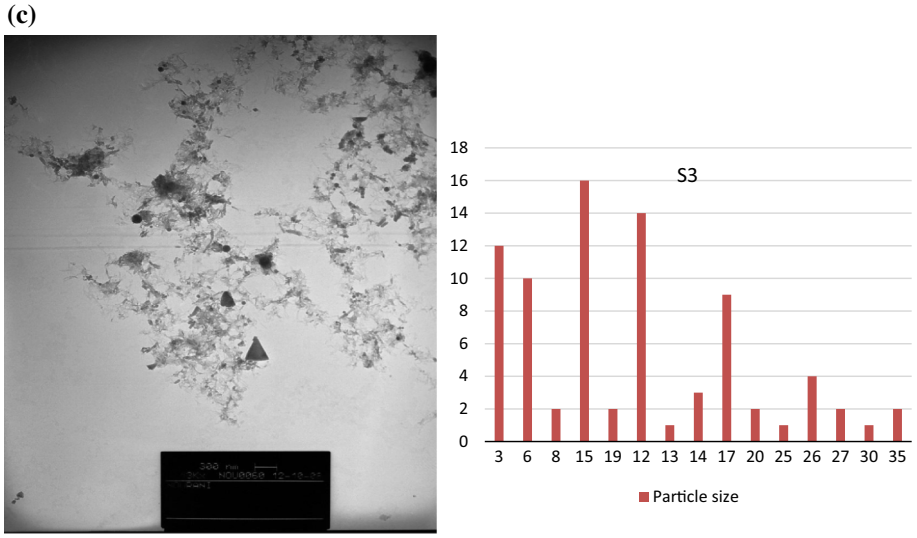

Fig. 2 continued

Results show that variation of transmission and reflection of Al doped PVA film depends on the concentration of doped nanoparticles rather than their size.

In Fig. 4b the refractive index of samples versus wavelength in the interval of 200–2000 nm is presented. For $\lambda > 400$ nm, the refractive index of thin films as almost independent of wavelength which was decreased with increasing the concentration of Al nanoparticles in their structure. There are a normal dispersion and anomalous dispersion regions for UV light. 200 nm $< \lambda <$ 340 nm the 340 nm $< \lambda <$ 400 nm are the anomalous and normal dispersion regions for Al NP doped PVA thin films respectively.

The optical absorption coefficients of samples are evaluated from the transmittance data using (Streetman 1990):

$$\alpha = \frac{1}{d} \ln \left[\frac{1}{T} \right] \tag{1}$$

where α is the absorption coefficient, T is the transmittance, and d is the thickness of samples, which was taken 0.07 mm. Figure 5 presents the optical absorption coefficients of pristine PVA and Al doped PVA samples. The absorption coefficient of films was

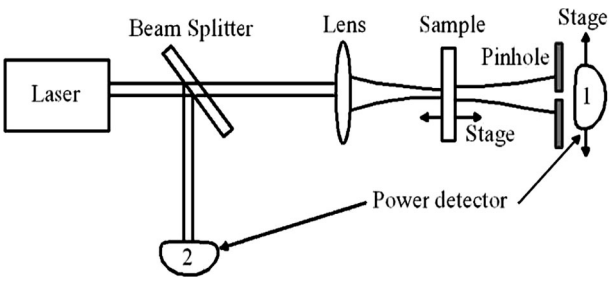

Fig. 3 Schematic diagram of experimental setup

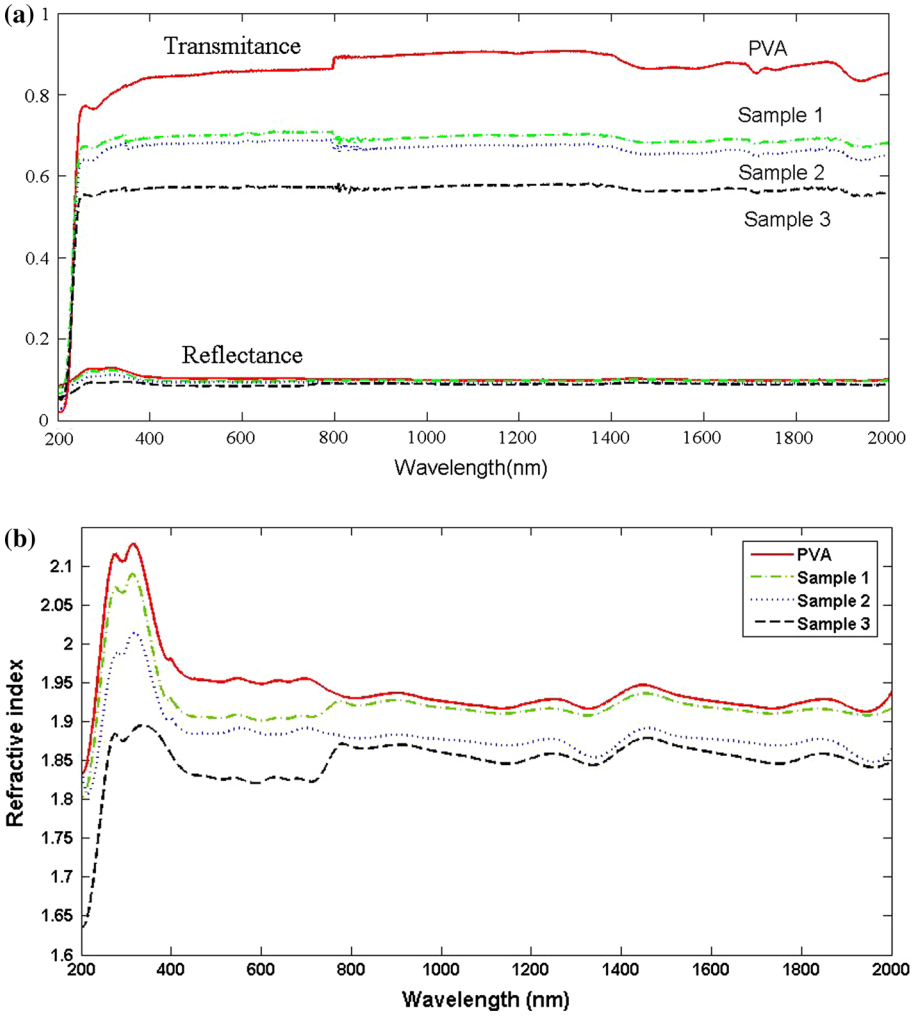

Fig. 4 **a** Optical transmittance and reflectance spectrum of samples, **b** reflective index of samples in NIR–Vis–UV spectrum

increased after doping nanoparticles in them. By increasing the concentration of doped nanoparticles in PVA films the absorption coefficient of samples were increased. Similar to transmission and absorption spectrum here also the absorption coefficient is under the influence of nanoparticles concentration rather than their size. The large absorption peak, appeared in UV range, is due to the energy gap of samples in this area. The position of the absorption edge was determined by extrapolating the linear portions of α versus $h\nu$ curves to zero absorption value. It is clear from Fig. 5 that the band edge showed a decrease with increasing the size of Al nanoparticles in the structure of films. The absorption edge shifted towards higher wavelength side, indicating the decrease in the optical band gap for the samples.

The most used method for estimation of the bandgap from optical measurement is the one proposed by Tauc et al. (1996). The optical bandgap of samples were deduced from the

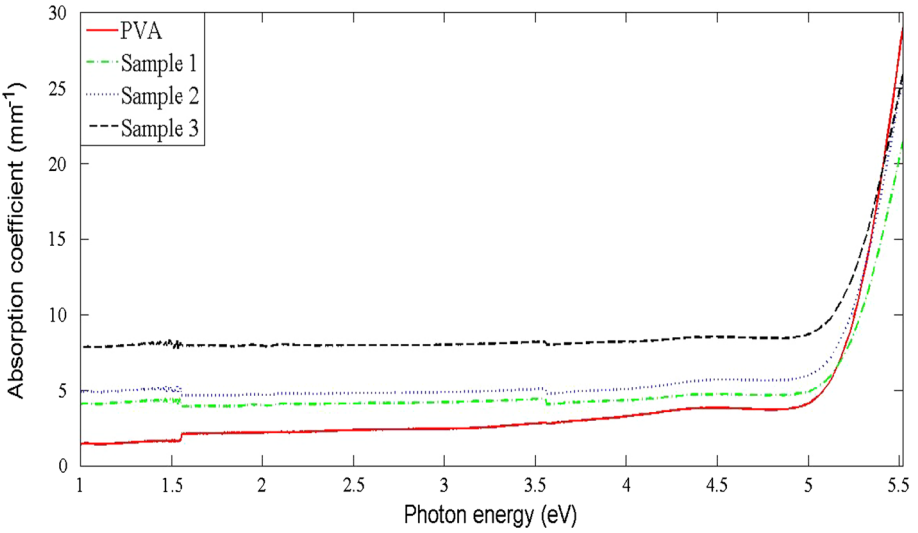

Fig. 5 Optical absorption coefficient of pristine PVA and doping samples

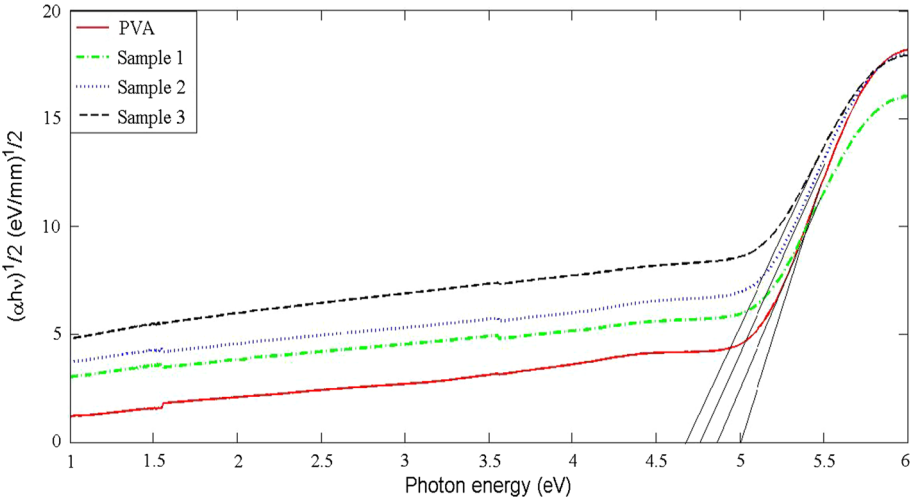

Fig. 6 $(\alpha h\nu)^{1/2}$ versus photon energy to illustrate Tauc method

intercept of the extrapolated linear part of the plot of $(\alpha E)^{1/2}$ versus the photon energy E with abscissa (see Fig. 6). This follows by the method of Tauc where:

$$\alpha E = B\left(E - E_g\right)^p \tag{2}$$

In this equation, α is the absorption coefficient, E is the photon energy, B is a factor that depends on transition probability and can be assumed to be constant within the optical frequency range and the index p is related to the distribution of the density of states is an index which assumes the values 1/2, 3/2, 2 and 3 depending on the nature of electronic transition. Taking $p = 2$, which selected by fitting method; the band gap energies of

samples were calculated. In an indirect gap, a photon cannot be emitted because the electron must pass through an intermediate state and transfer momentum to the crystal lattice. Bandgap energies of samples are presented in Table 1. Band gap energy of pure PVA film is extracted to be E_g (PVA) = 5.01 eV. In Ghanipour et al.'s report the bandgap energy of PVA films was 4.96 eV (Ghanipour and Dorranian 2015). Ghambari and Dorranian (2014) measured the band gap energy of PVA film to be about 5.4224 eV. In Ghorbani et al.'s work this magnitude was 4.95 eV (Ghorbani et al. 2016). As can be seen, the energy gap of samples is decreased noticeably from PVA to sample 3. E_g (S1) = 4.89 eV, E_g (S2) = 4.78 eV, and E_g (S3) = 4.69 eV, which is the effect of Al nanoparticles dopant. The band gap energy of samples decreased with increasing the concentration of nanoparticles in samples.

Optical properties, such as complex refractive indices for a certain range of wavelength between ultra violet and near infrared, are important criteria for the selection of fabricated films for various applications. Determination of the optical constants n and k is one of the most challenging tasks when studying the optical properties of materials, since this involves complex equations and a great deal of computing. A number of methods and different approaches exist to determine the optical constants of materials.

The complex refractive index is

$$n = n(\omega) + ik(\omega) \tag{3}$$

in which n is the real part and the extinction coefficient k, is the imaginary part. The refractive index n and the extinction coefficient k of the PVA films studied here were determined using the relation.

$$n = \frac{1+R}{1-R} + \sqrt{\frac{4R}{(1-R)^2} - k^2} \tag{4}$$

in which

$$k = \lambda\alpha/4\pi \tag{5}$$

The extinction coefficient k describes the properties of the material with respect to light of a given wavelength and indicates the amount of absorption loss when the electromagnetic wave propagates through the material. The data of refractive index n and the extinction coefficient k as a function of photon energy are shown in Fig. 7a, b (Zahedi and Dorranian 2013).

It can be discerned from Fig. 7a that the refractive index of Al nanoparticles doped PVA films is lower than the refractive index of pristine PVA and it decrease with increasing the concentration of Al nanoparticles in PVA matrix because samples become closer to conductors. This property is inherent in all conductors and due to localized fluctuation of charged particles in medium. Also decreasing value of refractive index may be an indication of low density of the films, which leads to an increasing of the inter-atomic spacing (Abdelaziz 2011). This is due to the formation of inter molecular hydrogen bonding between Al nanoparticles and the adjacent OH groups.

The extinction coefficient k describes the properties of the material with respect to light of a given wavelength and indicates the absorption changes when the electromagnetic wave propagates through the material. In the Fig. 7b, the extinction coefficient k of the doped samples is larger than the extinction coefficient of pristine PVA in the range of $h\nu < 5.2$ eV. And in this range k increased with increasing the amount of Al nanoparticles

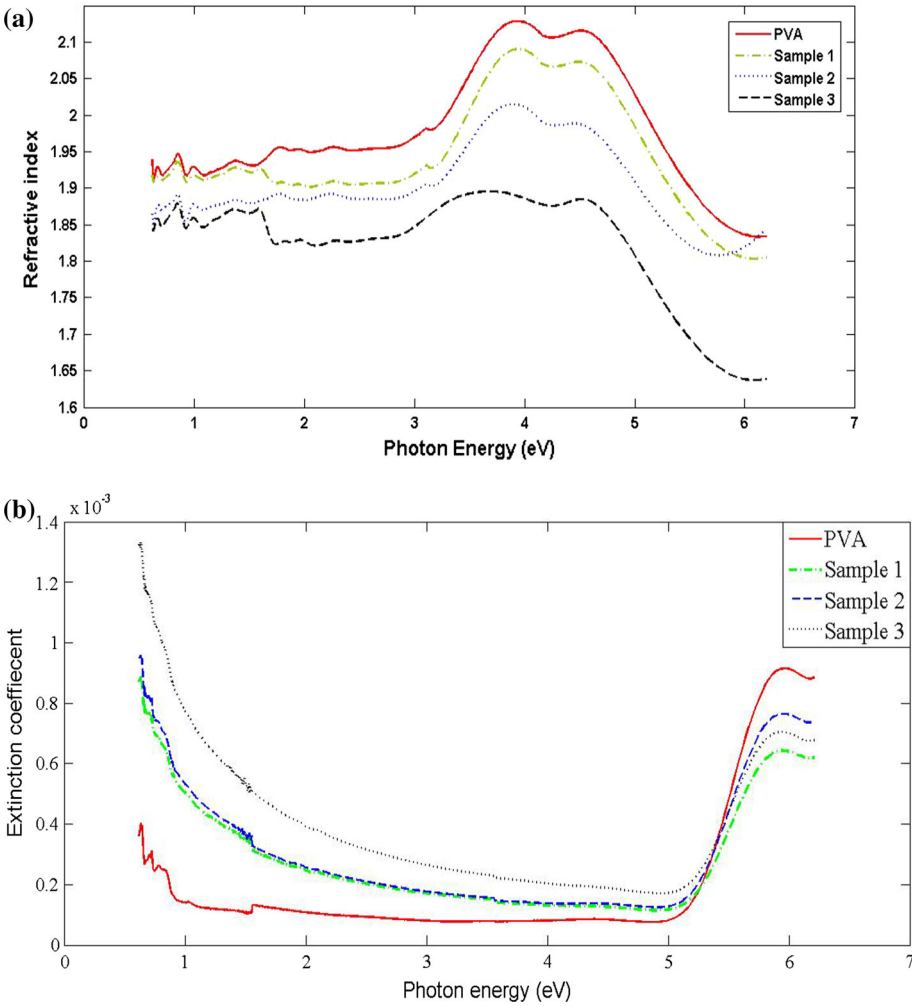

Fig. 7 **a** The refractive index in different photon energy for pure PVA and doping samples, **b** the extinction coefficient in different photon energy for pure PVA and doping samples

in the structure of the films. Results was inversed for the range of $h\nu > 5.2$ eV. This is the effect of metallic nanoparticle absorption. Bandgap energy of PVA is 5.01 eV. For $h\nu < 5.2$ eV the dominant mechanism of absorption is due to the presence of Al nanoparticles, while for the range of $h\nu > 5.2$ eV PVA absorbed the main part of photon energy.

Z-scan technique (Geethakrishnan and Palanysamy 2007; Sucharita et al. 2000), based on the spatial distortion of a laser beam passed through a nonlinear optical material (NLO), is widely used in material characterization because of its simplicity, high sensitivity and well-elaborated theory. The opportunity to conduct simultaneous measurements of various NLO parameters in one set of experiments also makes this technique attractive and applicable for different materials. This method produces both the sign and the magnitude of the nonlinearity. In addition, the value of the nonlinear refractive index n_2 may be easily

extracted from experimental data with a minimum of analysis (Geethakrishnan and Palanysamy 2007; Stepanov et al. 2003; Sheikh-Bahae et al. 1989). In the nonlinear regime, the absorption will be a nonlinear function of laser irradiance at a given point. In closed aperture Z-scan setup the transmitted intensity was measured through a pinhole in the far field as a function of the sample position (Z) that measured with respect to the focal plane. As the sample moves through the beam focus (Z = 0), self-focusing or defocusing modifies the detected beam intensity. For an open aperture Z-scan, pinhole is removed and transmitted beam touch the detector without any limitation. If the NLA coefficient (nonlinear absorption coefficient) (β) is positive, transmitted beam decreases with increase in the input laser irradiance (two photons absorption) and on the other hand, in the case of negative absorption it increases with increase in the input laser irradiance (saturation absorption).

In this paper, Z-scan technique was utilized to calculation of the NLA, NLR (nonlinear refractive) and third-order nonlinear electric susceptibility ($\chi^{(3)}$) with the procedure have been reported by Sheik-Bahae et al. previously (Sheikh-Bahae and Hasselbeck 2001). In Fig. 8a the closed aperture Z-scan data for pristine PVA, S1, S2 and S3 samples in

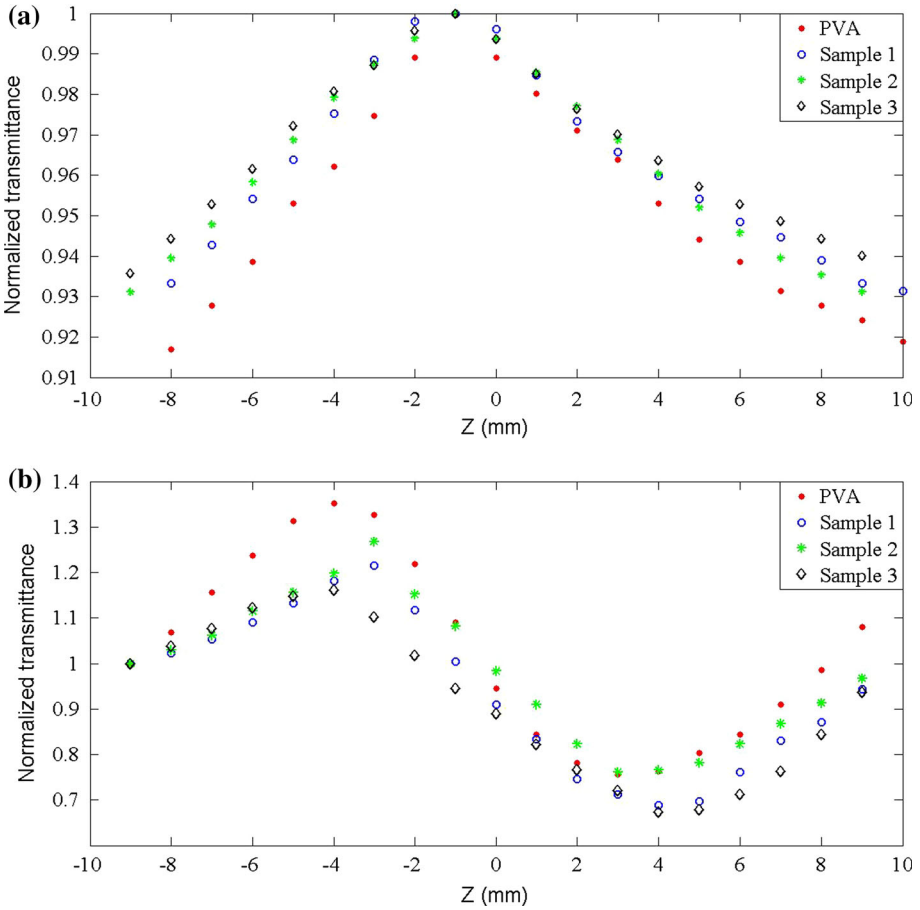

Fig. 8 **a** Open aperture Z-scan data for doped samples, **b** closed aperture Z-scan data for doped samples

$I_0 = 86.11 \times 10^3$ W/cm^2 have been presented (I_0 is the intensity of the laser beam at $z = 0$). The peak followed by a valley in normalized transmittance results indicates that the sign of the refractive index nonlinearity is negative, i.e. self-defocusing behavior. ΔT_{P-V} is the difference between normalized peak and valley transmittance values in closed aperture diagram. In this case, ΔT_{P-V} has been decreased with increasing the Al nanoparticle concentration in the nanocomposite films. Decreasing in ΔT_{P-V} cause to increase the absolute value of n_2 according to following equation:

$$n_2 = \frac{\Delta T_{P-V}\lambda}{0.406(1-S)^{0.25}2\pi I_0 L_{eff}} \tag{6}$$

where S is the linear transmittance of aperture given by following equation:

$$S = 1 - \exp\left(-2r_a^2/\omega_a^2\right) \tag{7}$$

That r_a is the radius of the aperture and ω_a is the beam waist on the aperture. S parameter was 0.5 for present experiment. I_0 is the intensity of the laser beam at focus point ($z = 0$) and was $I_0 = 86.11 \times 10^3$ W/cm^2 in this experiment. L is the thickness of nanocomposite films and L_{eff} is the effective thickness of the films and is equal:

$$L_{eff} = [1 - \exp(-\alpha L)]/\alpha \tag{8}$$

The α factor is linear absorption coefficient of the films and have been measured before. λ is the laser wavelength (532 nm).

As mentioned before, the NLA coefficient (β) can be calculated from the open aperture Z-scan data using following equations (Stepanov et al. 2003):

$$\beta = \frac{q_0}{IL_{eff}} \tag{9}$$

$$T_0 = q_0^{-1}\ln(1 + q_0) \tag{10}$$

where T_0 is the normalized transmittance in open aperture diagram and q_0 is the laser beam parameter at focal point. As we can see, (Fig. 8b) the open aperture curves behave a peak shape. This indicates a negative NLA coefficient. Whatever the nanoparticle concentrations increase in films, this peak increased. It seems that this behavior of the NLA in synthesized films can be attributed to saturation absorption mechanism (Sheikh-Bahae et al. 1989). The real and imaginary parts of third order susceptibility ($\chi 3$) are related to n_2 and β through following equations:

Table 2 Comparison of the value of n_2, β, and χ^3 of samples

Sample	$n_2 \times 10^{-8}$ (cm^2/W)	β (cm/W)	Re($\chi^{(3)}$) $\times 10^{-15}$ (esu)	Im($\chi^{(3)}$) $\times 10^{-14}$ (esu)	$\chi^{(3)}$ (esu)
PVA	−2.80	0.6465	−0.269	2.634	2.6477
Sample 1	−2.68	0.8168	−0.245	3.173	3.1824
Sample 2	−2.55	0.8431	−0.229	3.210	3.2181
Sample 3	−2.37	1.079	−0.197	3.814	3.8190

$$\mathrm{Re}\chi^{(3)}(\mathrm{esu}) = \frac{10^{-4}\varepsilon_0 c^2 n_0^2}{\pi} \times n_2(\mathrm{cm}^2/\mathrm{W}) \tag{11}$$

$$\mathrm{Im}\chi^{(3)}(\mathrm{esu}) = \frac{10^{-4}\varepsilon_0 c^2 n_0^2 \lambda}{4\pi^2} \times \beta(\mathrm{cm}^2/\mathrm{W}) \tag{12}$$

where n_0 is the linear refractive index, c is the light speed of free space. According to this theory, the results of the experiments were used to calculate n_2, β and $\chi^{(3)}$, which are presented in Table 2 for different synthesized nanocomposite films. According to these results, it seems that the values of n_2, β and $\chi^{(3)}$ (real and imaginary parts) have been increased with increasing Al NPs concentrations in the structure of thin films. The absolute value of NLR indices were decreased from 2.8×10^{-8} up to 2.37×10^{-8} cm^2/W and the NLA coefficients were enhanced from 0.6465 up to 1.079 cm/W with increasing of the Al NPs concentration in the films. Because of diffraction, the nonlinear refractive index is under the influence of the size of nanoparticles while because of absorption the nonlinear absorption coefficient varies proportional to the concentration of Al NPs. The comparable value of NLA coefficient was previously reported by Sharma et al. in in-situ synthesis of ZnSe/PVA nanocomposite (Sharma and Tripathi 2012). They founded the 4.52×10^{-5} cm/W and 2.62×10^{-11} m^2/V^2 values for NLA coefficient and nonlinear susceptibility respectively. The NLA coefficient for Au nanoparticles doped in PVA film was reported by Ghambari et al. They found that the NLA coefficient for PVA film doped with Au nanoparticles was decreased with increasing the size of nanoparticles (Ghambari and Dorranian 2014). The same results were reported by Ghanipour et al. They found the NLA and NLR coefficient for PVA film dopped with Ag nanoparticles (Ghanipour and Dorranian 2015). The nonlinearity of conductor NPs is often enhanced because of the surface plasmon resonance effect, especially when the wavelength of incident wave is close to the wavelength of their linear absorbance. One of the most important factors for increase of optical nonlinearity of Al/PVA nanocomposite films is the dielectric confinement effect. This effect depends on the dielectric constant ratio, which occurs when high refractive index NPs doped in low refractive index matrix or coated with a low refractive index film (Halajan et al. 2014). When Al NPs doped into PVA (possessing smaller dielectric coefficient) the electric charge interaction between them is strong so that the dielectric dipole film can be formed in the NPs surface. This effect is a surface polarization depending on the permittivity ratio between particles and surrounding medium. It can accelerate the separation of excited charges to enhance electric field inside nanoparticles. Thus, with increasing in NPs concentration, the enhancement of local electric field is responsible for enhanced nonlinear response in the nanocomposite films (Wang et al. 1994).

4 Conclusion

Nanocomposite films of Al NPs (with different concentrations) embedded in PVA were prepared and their nonlinear optical properties were studied. The Al NPs were synthesized by different fluence of laser pulse with pulsed laser ablation method in distilled water and combined with liquid PVA in water in equal weight percent. Solution was dried on a surface to produce 0.07 mm Al doped PVA films. The concentration of doped Al nanoparticles was increased from sample 1 to 3 while their sized was decreased.

Doping Al nanoparticles as conductor material in PVA films as an insulator decreased energy gap of samples. Results show that all linear optical parameter of films are under the

influence of nanoparticles concentration. In nonlinear regime the nonlinear refractive index increased with increasing the size of Al nanoparticles while the nonlinear absorption coefficient increased with increasing the concentration of Al nanoparticles in the structure of films. It can be explained using the mechanisms which are responsible for them. In the case of nanoparticles scattering is the main parameter for variation of nonlinear refractive index and absorption is the main parameter for variation of absorption coefficient.

References

Abbasi, M., Dorranian, D.: Effect of laser fluence on the characteristics of Al nanoparticles produced by laser ablation in deionized water. Opt. Spectrosc. **118**, 472–481 (2015)

Abdelaziz, M.: Cerium(III) doping effects on optical and thermal properties of PVA films. Phys. B **406**, 1300–1307 (2011)

Balde, C.P., Hereijgers, B.P.C., Bitter, J.H., de Jong, K.P.: Sodium alanate nanoparticles—linking size to hydrogen storage properties. J. Am. Chem. Soc. **130**, 6761–6765 (2008)

Catunda, T., Andreeta, J.P., Castro, J.C.: Differential interferometric technique for the measurement of the nonlinear index of refraction of ruby and $GdAlO_3$: $Cr(^{3+})$. Appl. Opt. **25**, 2391–2395 (1986)

Chen, S., Sommers, J.M.: Alkanethiolate-protected copper nanoparticles: spectroscopy, electrochemistry, and solid-state morphological evolution. J. Phys. Chem. B **105**, 8816–8820 (2001)

Fussell, G., Thomas, J., Scanlon, J., Lowman, A., Marcolongo, M.: The effect of protein-free versus protein-containing medium on the mechanical properties and uptake of ions of PVA/PVP hydrogels. J. Biomater. Sci. **16**, 489–503 (2005)

Galfetti, L., De Luca, L.T., Severini, F., Meda, L., Marra, G., Marchetti, M., Regi, M., Bellucci, S.: Nanoparticles for solid rocket propulsion. J. Phys. Condense Matter **18**, S1991–S2005 (2006)

Ganeev, R.A., Ryasnyanskii, A.I., Kodirov, M.K., Kamalov, S.R., Li, V.A., Tugushev, R.I., Usmanov, T.: Nonlinear optical parameters and optical limitation in cobalt-doped polyvinylpyrrolidone solutions. Technol. Phys. **47**, 991–995 (2002)

Geethakrishnan, T., Palanysamy, P.K.: Z-scan determination of the third-order optical nonlinearity of a triphenylmethane dye using 633 nm He–Ne laser. Opt. Commun. **270**, 424–428 (2007)

Ghambari, T., Dorranian, D.: Size effect of Au nanoparticles on the electrical and optical properties of PVA thin film. J. Nanoelectron. Optoelectron. **9**, 1–10 (2014)

Ghanipour, M., Dorranian, D.: Nonlinear optical characterization of the Ag nanoparticles doped in polyvinyl alcohol films. J. Opt. Spectrosc. **118**, 949–954 (2015)

Ghorbani, V., Ghanipour, M., Dorranian, D.: Effect of TiO_2/Au nanocomposite on the optical properties of PVA film. Opt. Quant. Electron. **48**, 61–62 (2016)

Halajan, M., Torkamany, M.J., Dorranian, D.: Effects of the ZnSe concentration on the structural and optical properties of ZnSe/PVA nanocomposite thin film. J. Phys. Chem. Sol. **71**, 1187–1193 (2014)

He, G.S., Yuan, L.X., Cui, Y.P., Prasad, P.N.: Studies of two-photon pumped frequency-upconverted lasing properties of a new dye material. J. Appl. Phys. **81**, 2529–2537 (1997)

Keirbeg, U., Vollmer, M.: Optical Properties of Metal Clusters, vol. 25. Springer, New York (1995)

Liu, K., Li, Y., Xu, F., Zuo, Y., Zhang, L., Wang, H., Liao, J.: Graphite/poly (vinyl alcohol) hydrogel composite as porous ringy skirt for artificial cornea. Mater. Sci. Eng. C **29**, 261–266 (2009)

Park, K., Lee, D., Rai, A., Mukherjee, D., Zachariah, M.R.: Size-resolved kinetic measurements of aluminum nanoparticle oxidation with single particle mass spectrometry. J. Phys. Chem. B **109**, 7290–7299 (2005)

Porel, S., Venkatram, N., NarayanaRao, D., Radhakrishnan, T.P.: In situ synthesis of metal nanoparticles in polymer matrix and optical limiting application. J. Nanosci. Nanotechnol. **7**, 1887–1892 (2007)

Roach, P.J., Woodward, W.H., Castleman Jr., A.W., Reber, A.C., Khanna, S.N.: Complementary active sites cause size-selective reactivity of aluminum cluster anions with water. Science **323**, 492–495 (2009)

Sharma, M., Tripathi, S.K.: Preparation and nonlinear characterization of zinc selenide nanoparticles embedded in polymer matrix. J. Phys. Chem. Sol. **73**, 1075–1081 (2012)

Sheik-Bahae, M., Hasselbeck, M.P. (eds.): OSA Handbook of Optics IV. McGraw-Hill, New York (2000)

Sheikh-Bahae, M., Hasselbeck, M.P.: Third order optical nonlinearities. In: Bass, M. (ed.) OSA Hand Book of Optics, vol. 17, pp. 17.3–17.38. McGraw-Hill, New York (2001)

Sheikh-Bahae, M., Said, A.A., Van Stryland, E.W.: High-sensivity, single-beam n_2 measurements. Opt. Lett. **14**, 955–957 (1989)

Stepanov, A.L., Ganeev, R.A., Ryasnyansky, A.I., Usmanov, T.: Non-linear optical properties of metal nanoparticles implanted in silicate glass. Nucl. Instrum. Methods Phys. Res. B **206**, 624–628 (2003)
Streetman, B.G.: Solid State Electronic Devices, 3rd edn, p. 309. Prentice Hall Inc., Englewood Cliffs (1990)
Sucharita, S., Alok, R., Dasgupta, K.: Solvent dependent nonlinear refraction in organic dye solution. J. Appl. Phys. **87**, 3222–3226 (2000)
Tauc, J., Grigorovici, R., Vancu, A.: Optical properties and electronic structure of amorphous germanium. Phys. Status Sol. **15**, 627–637 (1996)
Tingchao, H., Zhipen, C., Pengwei, L., Yongguang, C., Yujun, M.: Third-order nonlinear response of Ag/methyl orange composite thin films. J. Mod. Opt. **372**, 3937–3940 (2008)
Tyagi, H., Phelan, P.E., Prasher, R., Peck, R., Lee, T., Pacheco, J.R., Arentzen, P.: Generation of Al nanoparticles via ablation of bulk Al in liquids with short laser pulses. Nano Lett. **8**, 1410–1416 (2008)
Wang, J., Sheik-Bahae, M., Said, A.A., Hagan, D.J., Van Stryland, E.W.: Time-resolved Z-scan measurements of optical nonlinearities. J. Opt. Soc. Am. B **11**, 1009–1017 (1994)
Weickmann, H., Tiller, J.C., Thomann, R., Mulhhaupt, R.: Metallized organoclays as new intermediates for aqueous nanohybrid dispersions, nanohybrid catalysts and antimicrobial polymer hybrid nanocomposites. Macromol. Mater. Eng. **290**, 875–883 (2005)
Yang, G.W.: Laser ablation in liquids, application in the synthesis of nanocrystals. Prog. Mater. Sci. **52**, 648–698 (2007)
Yang, G., Guan, D.Y., Wang, W.T., Wu, W.D., Chen, Z.H.: The inherent optical nonlinearities of thin silver films. Opt. Mater. **25**, 439–443 (2004)
Yano, K., Usuki, A., Okada, A.: Synthesis and properties of polyimide–clay hybrid films. J. Polym. Sci. Part A **35**, 2289–2294 (1997)
Zahedi, S., Dorranian, D.: Effect of laser treatment on the optical properties of poly (methyl methacrylate) thin films. Opt. Rev. **20**, 36–40 (2013)
Zheng, S.Y., Fang, F., Zhou, G.Y., Chen, G.R., Ouyang, L.Z., Zhu, M., Sun, D.L.: Hydrogen storage properties of space-confined $NaAlH_4$ nanoparticles in ordered mesoporous silica. Chem. Mater. **20**, 3954–3958 (2008)